Dynamic and Sensitivity Analysis of KNTU CDRPM: A Cable Driven Redundant Parallel Manipulator

Mohammad M. Aref, Pooneh Gholami and Hamid D. Taghirad
Advanced Robotics and Automated Systems (ARAS),
Faculty of Electrical Engineering, K.N. Toosi University of Technology.

***Abstract*— KNTU CDRPM is a cable driven redundant parallel manipulator, which is under investigation for possible implementation of large workspace applications. This newly developed manipulators have several advantages compared to the conventional parable mechanisms. In this paper, the governing dynamic equation of motion of such structure is derived using the Newton-Euler formulation. Next, the dynamic equations of the system are used in simulations. It is shown that on the contrary to serial manipulators, dynamic equations of motion of cable-driven parallel manipulators can be only represented implicitly, and only special integration routines can be used for their simulations. In order to verify the accuracy and integrity of the derived dynamic equations, open– and closed–loop simulations for the system is performed and analyzed. Also, the effects of mechanical assembly tolerances on the closed–loop control performance of a cable driven parallel robot are studied in detail, and the sensitivity analysis of the precision in the construction and assembly of the system on the closed–loop behavior of the KNTU CDRPM is performed.**

I. Introduction

KNTU CDRPM is the name of a project defined on cable driven redundant parallel manipulator by ARAS (Advanced Robotics and Automated Systems) group of K. N. Toosi University of Technology. The main goal of this project is design, analysis and implementation of a universal parallel manipulator structure which uses cable driven actuators instead of any other type of linear actuators for a stiff, precise and high speed positioning task in a large workspace. The objective becomes more interesting in cases where the workspace is so wide that cannot be reached with usual serial manipulators. [1]. A rigid jointed parallel manipulator possess more stiffness and is capable to run at higher acceleration compared to that to a serial manipulator. However, as it is the case for many parallel mechanisms, a limited workspace with large singular regions within the workspace, is not a suitable solution for the above mentioned applications [2]. A spacious workspace with the capacity of high payload per moving mass can be easily achieved using a cable driven parallel mechanism. As an example in a large adaptive reflector (LAR) a $2km^2$ area can be manipulated with such mechanisms [3]. Nevertheless, one inherent limitation of any CDRPM is that the driven cables can apply only positive tension forces to the end–effector. To overcome this problem, in LAR application the end–effector is kept under high tension using a helium filled aerostat [4], while in the NIST RoboCrane design the problem is tackled by suspending the end-effector from the roof and using the gravity force [5]. These remedies are only applicable for applications with low acceleration and heavy moving platform. A more suitable solution is to achieve tension forces in the cables within the whole workspace, through an over–constrained structure [6]. In other words, by using additional cables compared to the required degrees of freedom, and carefully resolve the redundancy in order to keep all the cable forces in tension can significantly remedy the problem [7].

The design process of KNTU CDRPM consists of many steps and requires careful investigation in various perspectives. The basic step is the geometrical workspace analysis of the design. Kinematics and singularity analysis have significant role in the optimal assignment of the design parameters. Dynamic analysis provides the designer a tool to analyze and compare the dynamical behavior of different designs. Closed–loop performance of such mechanisms can be further analyzed using the dynamic simulation tool. Furthermore, the dynamic analysis can be used to perform a sensitivity analysis on the accuracy of different component, and the mechanical assembly to the final precision performance to the robot. In this paper the dynamic analysis of a cable driven redundant parallel manipulator is reported. Such analysis is an essential step to design such manipulators to guarantee the accomplishment of the required task, within its entire large workspace[8]. In order to perform dynamic analysis for such structures Newton–Euler formulation, the principle of virtual work, and Lagrange formulation can be used. The traditional Newton–Euler formulation has been used extensively in the literature to derive dynamic equations of general parallel manipulators [9], and also for the Stewart platform, which is the most celebrated parallel manipulator [10]. In this formulation all the reaction forces can be computed, which is very insightful for the design of KNTU CDRPM. On the

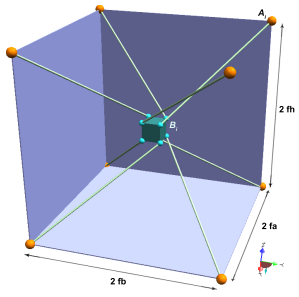

Fig. 1. The KNTU CDRPM, a Perspective View

1-4244-2367-5/08/$20.00 ©2008 IEEE

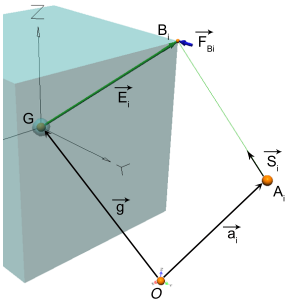

Fig. 2. ith Attachment point on the moving platform and related vectors

other hand, the equations of motion for each limb and the moving platform must be derived, which inevitably leads to a more extensive calculations.

It is shown that on the contrary to serial manipulators, dynamic equations of motion of parallel manipulators can usually be represented implicitly. Therefore, special integration routines are needed for the numerical integration of such equations. In order to verify the accuracy and integrity of the derived dynamics, open– and closed–loop simulations for the system is performed and analyzed. Moreover, the dynamical behavior of the manipulator is studied to validate the simulation results and to describe open–loop responses of the robot. Finally, in order to obtain an insightful tool to identify the significance of the construction and assembly procedure in the robot, a thorough sensitivity analysis is performed. In this analysis the contribution of the inaccuracy of the assembly of different components of the manipulator into the closed-loop performance is identified.

II. Kinematics

A. Mechanism Description

The KNTU Cable Driven Redundant Parallel Manipulator is illustrated in figure 1. This figure shows a spatial six degrees of freedom manipulator with two degrees of redundancy. This robot has eight identical cable limbs. The cable driven limbs are modeled as spherical-prismatic-spherical(SPS) joints, for cables can only bear tension force and not radial or bending force. Two cartesian coordinate systems $A(x, y, z)$ and $B(u, v, w)$ are attached to the fixed base and moving platform. Points $A_1, A_2, \ldots, A_8$ lie on the fixed cubic frame and $B_1, B_2, \ldots, B_8$ lie on the moving platform. The origin O of the fixed coordinate system is located at the centroid of the cubic frame. Similarly, the origin G of the moving coordinate system is located at centroid of the cubic moving platform. The transformation from the moving platform to the fixed base can be described by a position vector $\overrightarrow{g} = \overrightarrow{OG}$ and a 3×3 rotation matrix ${}^{A}R_{B}$. Consider a_i and ${}^{B}b_i$ denote the position vectors of points A_i and B_i in the coordinate system A and B, respectively. Although in the analysis of the KNTU CDRPM, all the attachment points, are considered to be arbitrary, the geometric and inertial parameters given in table I are used in the simulations.

B. Inverse Kinematics

Similar to other parallel manipulator, CDRPM has a complicated forward kinematic solution [11]. However, the inverse kinematic analysis is sufficient for dynamic modeling. As illustrated in figure 1, the B_i points lie at the vertexes of the cube. For inverse kinematic analysis of the cable driven parallel manipulator, it is assumed that the position and orientation of the moving platform $x = [x_G, y_G, z_G]^T$, ${}^{A}R_{B}$ are given and the problem is to find the joint variable of the CDRPM, $\boldsymbol{L} = [L_1, L_2, \ldots, L_8]^T$. From the geometry of the manipulator as illustrated in figure 2 the following vector loops can be derived:

$$ {}^{A}\overrightarrow{A_iB_i} + {}^{A}\overrightarrow{\boldsymbol{a}_i} = {}^{A}\overrightarrow{\boldsymbol{g}} + \boldsymbol{E}_i \tag{1} $$

in which, the vectors $\boldsymbol{g}, \boldsymbol{E}_i$, and $\boldsymbol{a}_i$ are illustrated in figure 2. The length of the i'th limb is obtained through taking the dot product of the vector $\overrightarrow{A_iB_i}$ with itself. Therefore, for $i = 1, 2, \ldots, 8$:

$$ L_i = \left\{ [\boldsymbol{g} + \boldsymbol{E}_i - \boldsymbol{a}_i]^T [\boldsymbol{g} + \boldsymbol{E}_i - \boldsymbol{a}_i] \right\}^{\frac{1}{2}} . \tag{2} $$

C. Jacobian

Jacobian analysis plays a vital role in the study of robotic manipulators.Let the actuated joint variable be denoted by a vector $\boldsymbol{L}$ and the location of the moving platform be described by a vector $\boldsymbol{x}$. Then the kinematic constrains imposed by the limbs can be written in the general form $\boldsymbol{f}(\boldsymbol{x}, \boldsymbol{L}) = 0$ by differentiating with respect to time, we obtain a relationship between the input joint rates and the end-effector output velocity as follows :

$$ J_x \dot{\boldsymbol{x}} = J_L \dot{\boldsymbol{L}} \tag{3} $$

where $J_{\boldsymbol{x}} = \frac{\partial \boldsymbol{f}}{\partial \boldsymbol{x}}$ and $J_{\boldsymbol{L}} = -\frac{\partial \boldsymbol{f}}{\partial \boldsymbol{L}}$. The derivation above leads to two separate Jacobian matrices Hence the overall Jacobian matrix J can be written as:

$$ \dot{\boldsymbol{L}} = \boldsymbol{J} \cdot \dot{\boldsymbol{x}} \tag{4} $$

where $\boldsymbol{J} = \boldsymbol{J}_L^{-1} \boldsymbol{J}_{\boldsymbol{x}}$. Jacobian matrix not only reveals the relation between the joint velocities $\dot{\boldsymbol{L}}$ and the moving platform velocities $\dot{\boldsymbol{x}}$, but also constructs the transformation needed to find the actuator forces $\boldsymbol{\tau}$ from the forces acting on the moving platform $\boldsymbol{F}$. When J_L is singular and the null space of J_L is not empty, there exist some nonzero $\dot{\boldsymbol{L}}$ vectors that result zero $\dot{\boldsymbol{x}}$ vectors which called serial type

TABLE I
Geometric and Inertial Parameters of the KNTU CDRPM

Description	Quantity
f_a: Fixed cube half length	$1\ m$
f_b: Fixed cube half width	$2\ m$
f_h: Fixed cube half height	$1\ m$
C : Cubic moving platform half dimension	$0.1\ m$
M: The moving platform's mass	$5\ Kg$
I: The moving platform's moment of inertia	$0.033\ Kg \cdot m^2$
ρ: The limb density per length	$0.007\ Kg/m$

singularity and when J_x becomes singular, there will be a non-zero twist rate $\dot{\boldsymbol{x}}$ for which the active joint velocities are zero. This singularity is called parallel type singularity [2]. In this section we investigate the Jacobian of the CDRPM platform shown in figure 1. For this manipulator, the input vector is given by $\boldsymbol{L} = [L_1, L_2, \ldots, L_8]^T$, and the output vector can be described by the velocity of the centroid G and the angular velocity of the moving platform as follows:

$$\dot{\boldsymbol{x}} = \begin{bmatrix} \boldsymbol{V}_G \\ \boldsymbol{\omega}_G \end{bmatrix} \tag{5}$$

Jacobian matrix of a parallel manipulator is defined as the transformation matrix that converts the moving platform velocities to the joint variable velocities, as given in equation 4. Therefore, the CDRPM Jacobian matrix $\boldsymbol{J}$ is a non-square 8×6 matrix, since the manipulator is a redundant manipulator. The Jacobian matrix can be derived by formulating a velocity loop-closure equation for each limb. Thus, the CDRPM Jacobian matrix $\boldsymbol{J}$ is derived as following [12].

$$\boldsymbol{J} = \left[\begin{array}{c|c} \hat{\boldsymbol{S}}_1^T & (\boldsymbol{E}_1 \times \hat{\boldsymbol{S}}_1)^T \\ \hat{\boldsymbol{S}}_2^T & (\boldsymbol{E}_2 \times \hat{\boldsymbol{S}}_2)^T \\ \vdots & \vdots \\ \hat{\boldsymbol{S}}_8^T & (\boldsymbol{E}_8 \times \hat{\boldsymbol{S}}_8)^T \end{array}\right] \tag{6}$$

in which, $\hat{\boldsymbol{S}}_i$ is the unit vector along i'th cable.

III. Dynamic Analysis

A. Kinetics

The main approach of dynamic analysis of CDRPM is Newton-Euler method. In this approach the free-body diagrams of each component is considered separately. The Newton-Euler equations are applied to all limbs and moving platform containing external, contact and inertia forces or torques. It is assumed that the moving platform center of mass is located at the geometrical center point G and it has a mass of M and moment of inertia I_G. Furthermore, since the manipulator is cable-driven, the mass of the limbs depend on cable length, $m = \rho L_i$ in which the cables have circular cross section, and a constant density per unit length of ρ. Thus, the cables' moments of inertia are varying, and can be calculated assuming that they are slender bars with circular cross section and with varying length as illustrated in figure 3. Non–zero elements of the moment of inertia of the cables about the fixed point A_i is given by:

$$I_{\text{yy}} = I_{\text{zz}} = \frac{1}{3}\rho L_i \tag{7}$$

The velocity vector of the center of mass of each limb consists of rotational and linear elements:

$$\boldsymbol{v}_{\text{ci}} = \frac{1}{2}(\dot{L}_i \hat{\boldsymbol{S}}_i + L_i \omega_i \times \hat{\boldsymbol{S}}_i) \tag{8}$$

The Newton-Euler equations for varying mass cable can be written as:

$$\sum \boldsymbol{F}_{\text{ext}} = \frac{\partial}{\partial t}(m_i \boldsymbol{v}_{\text{ci}}), \quad \sum \boldsymbol{M}_{\text{Ai}} = \frac{\partial}{\partial t}(I_{\text{Ai}} \boldsymbol{\omega}_i) \tag{9}$$

Hence,

$$\begin{aligned} \boldsymbol{F}_{\text{Bi}} &= \boldsymbol{F}_{\text{Ai}} - \frac{\rho}{2}\left(\dot{L_i}^2 + \ddot{L}_i L_i\right) \\ &\quad -\frac{\rho}{2} L_i^2 \left[\dot{L}_i \boldsymbol{\omega}_i \times \hat{\boldsymbol{S}}_i + \dot{\boldsymbol{\omega}}_i \times \boldsymbol{S}_i + \omega_i \times (\boldsymbol{\omega}_i \times \hat{\boldsymbol{S}}_i)\right] \end{aligned} \tag{10}$$

in which, $\ddot{L}_i$ and $\dot{\boldsymbol{\omega}}_i$ are linear and angular accelerations of i'th limb. Unfortunately, they depend on the acceleration of the end–effector. This dependency causes implicit differential equations of motion. By using light weight cables such as the ones used in this manipulator, the gravity force effects on the cables can be ignored compared to the dynamic induced forces [13]. As shown in figure 3, F_{Ai}^S the cable's tension force applied by cable driver unit can be represented by $\boldsymbol{F}_{\text{Ai}}^S = -\boldsymbol{\tau}_{\text{Ai}}$. Relations between actuator forces and the end-effector affected forces had been studied in cable-affected forces. Writing the Newton-Euler equations for moving platform, describes the relation between forces, torques and acceleration of moving platform as following:

$$\boldsymbol{M}\ddot{\boldsymbol{x}} = \boldsymbol{F}_D + \boldsymbol{G} + \sum_{i=1}^{n} \boldsymbol{F}_{\text{Bi}} \tag{11}$$

$$\boldsymbol{I}_G \ddot{\boldsymbol{\theta}} = \boldsymbol{\tau}_D - \sum_{i=1}^{n} \boldsymbol{E}_i \times \boldsymbol{F}_{\text{Bi}} \tag{12}$$

In which, $\boldsymbol{M}$ and $\boldsymbol{I}_G$ are moving platform's mass and moment of inertia and n is the number of the cables. $\boldsymbol{G}$ is the effect of the gravity force on the end-effector, $\boldsymbol{F}_D$ and $\boldsymbol{\tau}_D$ are the disturbance forces and torques acting on the moving platform with respect to the fixed frame coordinate. Equations 11 and 12 can be viewed as an implicit 6×1 set of differential equations as a relation between position $\boldsymbol{x}$, velocity $\dot{\boldsymbol{x}}$, acceleration $\ddot{\boldsymbol{x}}$, disturbance wrench $\mathfrak{F}_D$ and actuators torque $\boldsymbol{\tau}$ of the form:

$$\boldsymbol{f}_f(\boldsymbol{x}, \dot{\boldsymbol{x}}, \ddot{\boldsymbol{x}}, \mathfrak{F}_D, \boldsymbol{\tau}) = 0 \tag{13}$$

The use of these equation is twofold. The first use of it is to evaluate the actuator forces τ needed to produce a prescribed trajectory $\boldsymbol{x}(t)$ in presence of the disturbance wrench $\mathfrak{F}_D$. However, the governing equations of motion of the manipulator can be implemented for dynamic simulation of the system. For dynamic simulation, it is assumed that the actuator forces $\boldsymbol{\tau}(t)$, are given and the manipulator motion trajectory $\boldsymbol{x}(t)$, is needed to be determined. Due to implicit nature of the dynamic equation special integration routine

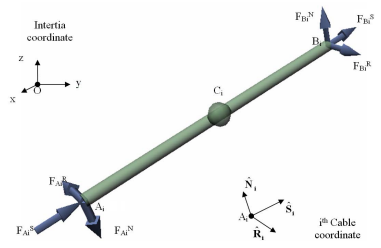

Fig. 3. ith Cable's moving coordinate and force elements

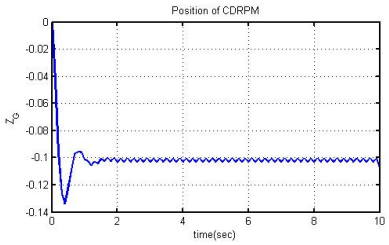

Fig. 4. Response of the dynamic model while actuator forces have same magnitude.

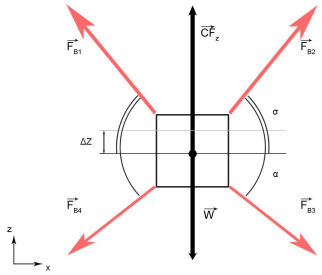

Fig. 5. The same actuator forces are applied: the sum is nonzero.

capable of integrating implicit differential equations, are used for simulations.

B. Model Verification

As explained before, the most important application of the dynamic equations of the CDRPM is the direct dynamic simulation of the system. In this case, it is assumed that the actuator forces are given and the manipulator motion is to be determined. Due to implicit nature of the dynamic equation, usual numerical integration routines such as Runge–Kutta methods [14], cannot be used to solve the problem. However, special integration routine[15], which is capable to integrate implicit functions, can be used for dynamic simulations. Simulations are performed to first verify the derived dynamic equations and then to study the behavior of the system. Thus, the model is simulated in some scenarios in which the behavior of the system can be predicted by intuition.

In order to study the cable constrained motion of the moving platform, all tension forces of the cables $\boldsymbol{\tau}_{Ai}$ are set to $100N$. In order to describe the simulated behavior of the system, it is simpler to consider only the front view of CDRPM as shown in figure 5. In this scenario, the initial geometry of the moving platform is symmetric with respect to the x, y, and z axes, and all actuator forces acting on the moving platform have the same size. Therefore, the forces and torques are balanced statically and the resultant force acting on moving platform is zero. The simulation results confirms the static balance of the manipulator in this case. Nevertheless, when any other force or displacement disturbance is applied, statical equilibrium is disturbed, and as illustrated in figure 5, in which $\overrightarrow{W}$ is the gravity force effect on the moving platform, changes the force balance. In this case, the resultant force $\boldsymbol{CF}_z$, is in the z direction and the resulting motion is shown in figure 4.

$$\boldsymbol{CF_z} = \sum_{\boldsymbol{i=1}}^{\boldsymbol{8}} \boldsymbol{F}^{\boldsymbol{z}}_{\mathrm{Bi}} \tag{14}$$

The magnitude of the resulting force can be derived as:

$$\mathrm{CF}_z = 2\sum_{i=1}^{4} {}^{B}F^{S}_{\mathrm{Bi}}(\sin(\sigma) - \sin(\alpha)) \tag{15}$$

Where the angles σ and α are shown in figure 5, and σ is measured counter clockwise and α is measured clockwise. Using the manipulator geometry, it can be shown that sinusoid of the angles σ and α are a function of only the z variable as following:

$$\sin(\sigma) = \frac{f_{fix} - z}{\mathrm{Li}} \;\; ; \;\; \sin(\alpha) = \frac{f_{fix} + z}{\mathrm{Li}}, \tag{16}$$

since, F^{S}_{Bi} forces have the same magnitudes while accelerations are small. Substituting equations 16, in equation 15, the Newton-Euler equations in z direction can be simplified into the following differential equation:

$$M\ddot{z} = CF_z - W \tag{17}$$

collecting all fixed coefficients, and replacing them with two constant parameter K_o, and K_1 simplifies the dynamic equation into:

$$M\ddot{z} = k_o - k_1 z \tag{18}$$

Thus, the system behaves similar to a free vibrating system in z direction without damping. As shown in figure 4, the simulation results of the dynamical model verifies a free vibration in z direction. Similar scenarios are simulated in order to verify the dynamic behavior of the system, and in all cases similar correspondences are observed.

C. Verification of Cable Modeling

In the dynamical simulation equations, the cable driven limbs are modeled as slender bars. However, in practice the cables can only bear tension force and neither radius nor bending forces can be transmitted through cables. In order to exactly model the cables, a finite element approach can be performed [16]. This examination makes the modeling too complicated, and unsuitable for further inverse dynamics control development. The over-constrained design of the manipulator, and using two degrees of redundancy in actuation,

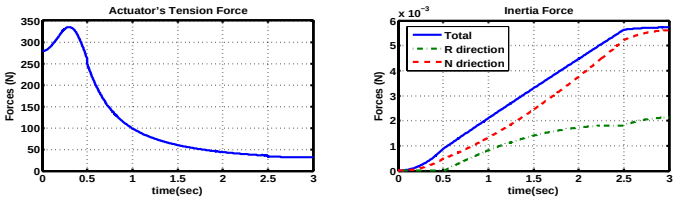

Fig. 6. In comparison to tension forces, inertia terms of the cables are much smaller.

makes the overall stiffness of the system higher than fully-constrained mechanism. Thus, if the force distribution is well conditioned, the tension forces in the cables must be much higher than the bending forces. Dynamic simulations can be used to verify this issue in more detail. If this is true the assumption of considering cables as slender bars will cause negligible effect into the true dynamics of the system.

As shown in figure 6, the amounts of the radial forces on the cables, are less than $\%0.1$ of the tension forces applied through the cables, while the end-effector has about $0.5^{m}/_{s^2}$ acceleration. Also it is valuable for the designer to know each attachment point has to carry about $340N$ along each cable for aforementioned acceleration of end-effector in all 3 axes.

IV. Sensitivity Analysis

As shown in figure 7, a joint space controller is proposed to examine the closed–loop performance of the dynamic model. Since there is no measurement available from the actual position of the end-effector, in this proposed controller the control law depends only on the cable length measurements and the desired trajectory. A full description of this paper is given in [17].

High precision requirements make the process of construction and assembly of the robots more stringent and expensive [18]. On the other hand, most of the production methods have their own inherent limitations in terms of production tolerances. On the other hand, the exact location of the attachment points at both fixed and moving frames can significantly affect the KNTU CDRPM's kinetic and dynamic behavior and the overall closed–loop performance. It is essential to notice that, the position and direction of the cable in the attachment point cause the direction of actuated force on the end-effector. Sensors range is too small to cover the large workspace of a CDRPM [2], [19]. Therefore, usually the desired position is used as the basis for evaluation of the Jacobian instead of the actual measurements in the practical implementation of the proposed control law. Therefore, it is essential to analyze the dynamic behavior of the robot in presence of such construction and assembly tolerances. Therefore, in order to obtain a pre–defined and repeatable precision for the end-effectors movements, in this section we will obtain an acceptable tolerance region around the attachment points that can fulfill the required closed–loop performance. This tolerance region is denoted as *allowed tolerance sphere* (ATS) which has a radius of r_{ATS} for the fixed frame's attachment points, A_is, and s_{ATS} the moving

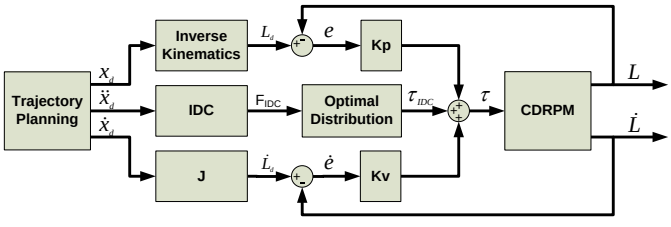

Fig. 7. Block diagram of the Closed–Loop system

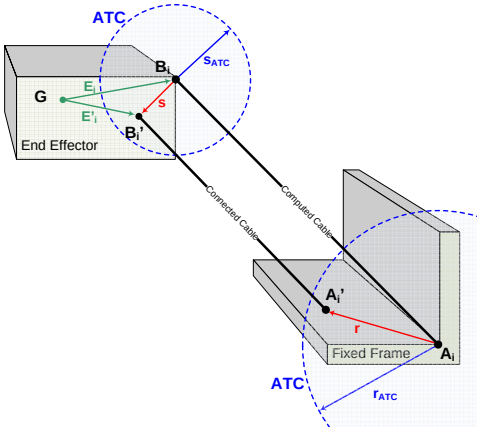

Fig. 8. Generated alternative points

frame's attachment points, E_is. Note that, all the induced errors are caused because of calculation errors. Other sources of errors such as the actuator and the other mechanical and measurement errors may be added to the induced errors.

A typical trajectory is considered for this analysis as introduced in [17]. A point inside of the fixed frame's ATS is assumed as A'_i and a point inside of the moving frame's ATS is assumed as B'_i as shown in figure 8.

For, the position vectors of the new points become:

$$\overrightarrow{a'_i} = \overrightarrow{a_i} + \vec{r}\ ,\ \overrightarrow{E'_i} = \overrightarrow{E_i} + \vec{s} \tag{19}$$

$\overrightarrow{r}$ and $\overrightarrow{s}$ are homogenous distributed random generated vectors, inside of the ATS region of the fixed and the moving attachment points:

$$\|\vec{r}\| < r_{ATS}\ ,\ \ \|\vec{s}\| < s_{ATS}$$

Thus, the inverse kinematics formulation is changed from equation 2 into:

$$L'_i = \left\{[\boldsymbol{g} + \boldsymbol{E'_i} - \boldsymbol{a'_i}]^T[\boldsymbol{g} + \boldsymbol{E'_i} - \boldsymbol{a'_i}]\right\}^{\frac{1}{2}} \tag{20}$$

And alternative Jacobian becomes:

$$\boldsymbol{J'} = \begin{bmatrix} \hat{\boldsymbol{S}'}_1^T & (\boldsymbol{E'_1} \times \hat{\boldsymbol{S}'}_1)^T \\ \hat{\boldsymbol{S}'}_2^T & (\boldsymbol{E'_2} \times \hat{\boldsymbol{S}'}_2)^T \\ \vdots & \vdots \\ \hat{\boldsymbol{S}'}_8^T & (\boldsymbol{E'_8} \times \hat{\boldsymbol{S}'}_8)^T \end{bmatrix} \tag{21}$$

Where $\hat{\boldsymbol{S}}'_i$ is the alternative unit vector calculated using A'_i and B'_i position instead of A_i and B_i. Therefore, after replacing all phrases in the equations 1 to 12, the alternative points, vectors and all changed equations that affect the dynamic simulation blocks is included in the simulations. The resulting simulation errors are shown in figure 9 where, the attachment points are modified by $\overrightarrow{r}$ and $\overrightarrow{s}$. Through this simulation, the computed radius of ATS is 3 mm for the moving attachment points and 12 mm for the fixed attachment points, in order to retain the desired precision of 0.015 mm error norm for position and $0.005°$ error norm

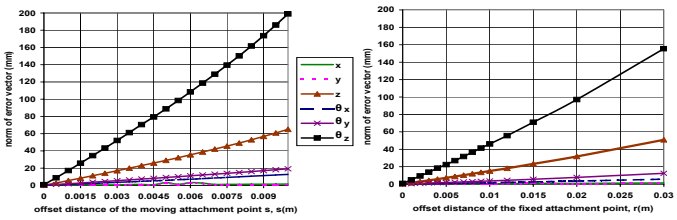

Fig. 9. Effect of attachment points change on the norm 2 of tracking error

for orientation. Let's break down the two norm of the error vector with respect to the components of the tolerances in position and orientation of the attachment points. The error is generated from the difference of the closed–loop simulation output and the corresponding desired position. By increasing $\boldsymbol{r}$ or $\boldsymbol{s}$ the norm of the error will be increasing as shown in figure 9. The norm of the error is decomposed by the position and orientation tolerances in the attachment points. As it is seen in this figure, the resulting tracking error is more sensitive to the tolerances experienced in the moving attachment point compared to that of the fixed attachment points. Fortunately, the end-effector's attachment points B_i's, are usually much closer to each other than the fixed attachment points. Thus, a CMM (Coordinate-measuring machine) [20] or any ordinary calibration tool should be used to ensure the required tolerances in the $\boldsymbol{E}_i$. Furthermore, it is seen that the resulting tracing error is also more sensitive to the orientation errors compared to that to the position errors. This is more critical for the tolerances in z axis orientation. Thus, if there exists any offset of end of arm tooling from the moving platform, precision of positioning will be affected specially in z direction.

V. Conclusions

In this paper, the dynamic analysis of the KNTU CDRPM is studied in detail. This manipulator is a cable driven redundant parallel manipulator, which is under investigation for possible high speed applications. Dynamic analysis is an essential step to design such manipulators in a way to accomplish the required performance within its entire workspace. In this analysis the inverse kinematics and Jacobian matrices of the manipulator is derived first. Then the motion equations of the manipulator are derived using Newton–Euler formulation. In this formulation all the reaction forces can be computed, which is very insightful for the design of the CDRPM. In order to verify the integrity and the accuracy of the dynamic equations, cable model is verified. Then, a simulation study is performed on the system for the open– and closed–loop scenarios. The integrity of the models are verified through the open–loop simulations, while it is shown that a decentralized PD controllers are able to reduce the induced vibration caused by the cable structures in these manipulators. It is shown that the obtainable tracking performance is less than 0.1 mm in position and less than 0.05^o in orientation. The dynamic simulations are finally used to examine the effect of construction and assembly tolerances to the closed–loop performance of the system. It is shown that if a 0.015 mm error for position and a 0.005° error for orientation is required, the radius of the allowed tolerance sphere for the fixed attachment points (A_i) is $r_{ATS} = 0.012m$ and that for the moving attachment points is $s_{ATS} = 0.003m$. Thus, performance of close–loop is four times more sensitive to the accuracy of the B_i points than that of the fixed A_i attachment points. A rationale behind this observation is the exitance of $\boldsymbol{E}_i$ terms in the Jacobian matrix and its effect on the applied torque of the end-effector noting that the vector ($\hat{\boldsymbol{S}}_i$) is normalized. Thus, a change in the size or direction of $\boldsymbol{E}_i$ has direct effect on the direction of $\hat{\boldsymbol{S}}_i$ and on the Jacobian's elements $\boldsymbol{E}_i \times \hat{\boldsymbol{S}}_i$ size and direction. While a change in the $\boldsymbol{a}_i$ will only influence the direction of $\hat{\boldsymbol{S}}_i$. Furthermore, it is shown that the most significance factor in the assembly of the attachment points is the z axis orientation precision.

References

[1] C. Ahn, T. Seo, J. Kim, and T. wan Kim, "High-tilt parallel positioning mechanism development and cutter path simulation for laser micro-machining," *Computer-aided Design Journal*, vol. 39, 2007.

[2] J. Merlet, *Parallel Robots*. Springer, 2006.

[3] H. D. Taghirad and M. Nahon, "Kinematic analysis of a macro-micro redundantly actuated parallel manipulator," *Advanced Robotics*, 2008.

[4] D. Wang and M. Meng, "Mobility analysis of the large adaptive reflector antenna reflector," in *Canadian Conference on Electrical and Computer Engineering*, vol. 2, pp. 865–869, 2000.

[5] S. E. Landsberger and T. Sheridan, "A new design for parallel link munipulator," *Proc Systems, Man and Cybernetics*, pp. 8–12, 1985.

[6] C. Pham, S. Yeo, G. Yang, M. Kurbanhusen, and I. Chen, "Force-closure workspace analysis of cable-driven parallel mechanisms," *Mechanism and Machine Theory*, pp. 53–69, 2006.

[7] O. So-Ryeok and S. Agrawal, "Generation of feasible set points and control of a cable robot," *IEEE Trans. on Robotics*, vol. 22, pp. 551–558, January 2006.

[8] M. Aref and H. Taghirad, "Geometrical workspace analysis of a cable-driven redundant parallel manipulator: KNTU CDRPM," in *IEEE Int.Conf. IROS*, 2008.

[9] C.Gosselin, "Parallel computational algorithms for the kinematics and dynamics of planar and spatial parallel manipulators," *Trans. ASME Journal of Dynamic Systems, Measurement and Control*, pp. 22–28, 1996.

[10] N. Dasgupta and T. Mruthyunjaya, "A newton-euler formulation for the inverse dynamics of the stewart platform manipulator," *Mechanism and Machine Theory*, 1998.

[11] S. Song and D. Kwon, "Geometric formulation approach for determining the actual solution of the forward kinematices of 6-dof parallel manipulators," in *IEEE Int. Conf. IROS*, pp. 1930–1935, 2002.

[12] P. Gholami, M. M. Aref, and H. D. Taghirad, "Dynamic analysis of the KNTU CDRPM: a cable driven redundant manipulator," in *Int. Conf. ICEE2008*, (Iran, Tehran), 2008.

[13] X. Diao and O. Ma, "Workspace analysis of a 6-dof cable robot for hardware-in-the-loop dynamic simulation," in *IEEE/RSJ Int.Conf. IROS*, 2006.

[14] L. F. Shampine, *Numerical solution of ordinary differential equations*. Chapman & Hall, 1994.

[15] L. Shampine, "Solving 0=f(t, y(t), y'(t)) in matlab," *Journal of Numerical Mathematics*, vol. 10, no. 4, pp. 291–310, 2002.

[16] G. Meunier, B. Boulet, and M. Nahon, "Control of an overactuated cable-driven parallel mechanism for a radio telescope application," *to appear in IEEE Transactions on Control Systems Technology*, 2008.

[17] P. Gholami, M. Aref, and H. Taghirad, "On the control of the KNTU CDRPM: A cable driven redundant parallel manipulator," in *IEEE/RSJ Int. Conf. IROS*, 2008.

[18] M. Hiller, S. Fang, S. Mielczarek, R. Vehoeven, and D. Franitza, "Design, analysis and realization of tendon-based parallel manipulators," *Mechanism and Machine Theory*, pp. 429–445, 2005.

[19] K. Varadarajan and M. Culpepper, "A dual-purpose positioner-fixture for precision six-axis positioning and precision fixturing," *Precision Engineering*, vol. 31, no. 3, pp. 276–286, 2007.

[20] Bosch, *Coordinate Measuring Machines and Systems*. CRC, 1995.